Astron. Astrophys. 315, L281–L284 (1996)

ASTRONOMY
AND
ASTROPHYSICS

H_2 infrared line emission from S140: a warm PDR⋆

R. Timmermann[1], F. Bertoldi[1], C.M. Wright[1], S. Drapatz[1], B.T. Draine[2], L. Haser[1], and A. Sternberg[3]

[1] Max-Planck-Institut für Extraterrestrische Physik, Giessenbachstraße, D-85740 Garching, Germany
[2] Princeton University Observatory, Peyton Hall, Princeton, NJ 08544, USA
[3] School of Physics and Astronomy, Tel Aviv University, Ramat Aviv 69978, Israel

Received 15 July 1996 / Accepted 7 August 1996

Abstract. ISO SWS spectra of H_2 pure rotational and ro-vibrational transitions, as well as [FeII], and [SiII] fine structure lines were obtained for one position on the photodissociation region (PDR) adjacent to the bright rim of the S140 HII region. The gas density is $\approx 10^4$ cm^{-3} and the incident UV flux $\chi \approx 400$ at the location of the ionization front. Our PDR model analysis shows that the relative H_2 line intensities are characteristic of low-density fluorescent emission and that the gas temperature is $T > 500$K in the partially dissociated gas. A comparison of predicted and observed fine structure line intensities permits an estimate of the abundances of Fe and Si.

Key words: ISM: individual: S140 – reflection nebulae – molecules – abundances – HII regions – infrared: ISM: lines and bands

1. Introduction

Among the first objects examined with the ISO short wavelength (2.4–45μm) spectrometer (SWS) within our program to study the physics of warm, dense molecular gas is the photodissociation region adjacent to the prominent bright rim (Blair et al. 1978) of the S140 HII region. Here a dense clump in the L1202/L1204 molecular cloud (Minchin et al. 1995) is exposed to ionizing and dissociating radiation from a nearby B0.5V star, resulting in strong emission of rotational and ro-vibrational lines of H_2 and of ionic fine structure lines. ISO has extended the wavelength range within which H_2 line emission can be observed to include many prominent near and mid IR lines, in particular those arising from transitions within the vibrational ground state. Observations that include those as well as ro-vibrational transitions from higher v yield important clues to the physical state of the gas, and the dissociation, excitation and formation properties of H_2.

Send offprint requests to: F. Bertoldi (MPE)

⋆ Based on observations with ISO, an ESA project with instruments funded by ESA Member States (especially the PI countries: France, Germany, The Netherlands and the United Kingdom) and with the participation of ISAS and NASA. The SWS is a joint project of SRON and MPE.

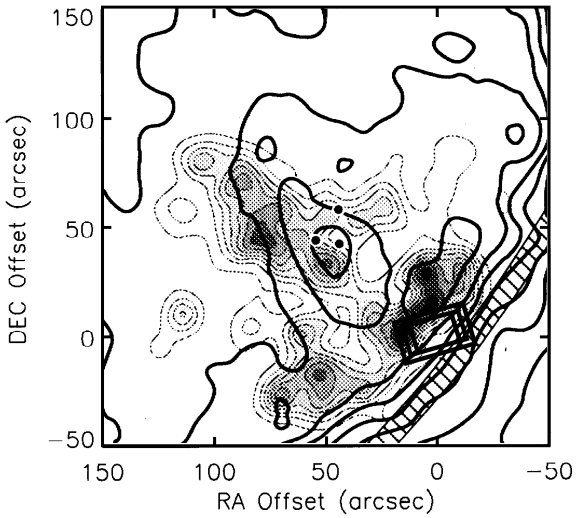

Fig. 1. Positioning of the SWS aperture ($\lambda < 12\mu$m: $14'' \times 20''$, $12 - 29.5\mu$m: $14'' \times 27''$, $\lambda > 29.5\mu$m: $20'' \times 30''$; long axis 106° E of N) relative to emission of CO(3-2) (contours), [CI] (greyscale), and the ionization front (shaded) [map from Hayashi et al. 1992].

2. Observation

Our pointing, $22^h17^m35^s.0$, +63°03′01″ (1950), coincides with the inner edge of the Hα (Hayashi et al. 1985) and radio continuum (Schwartz 1985) peak emission, and with the outer edge of the CO (Hayashi et al. 1987) emission and the [CI]609μm (White & Padman 1991) emission ridge (Fig. 1). Recent [CII]158μm observations by Schneider et al. (1992) locate our pointing on the peak of the [CII] emission ridge, which runs parallel in between the ionized gas rim and the [CI] emission rim. Since the H_2 emission in PDRs originates from the gas in between the hydrogen ionization front and the warm CI layer behind the CO dissociation front, our observing position appears to cover the expected location of the H_2 dissociation front. Our pointing also coincides with a steep rise in the CO excitation temperature to about 250K (Minchin et al. 1993: Fig. 13, offset position 63″). The clear separation between the apparently limb-brightened emission ridges of [CI], [CII], and Hα suggests a near edge-on view of a thin and slightly curved PDR.

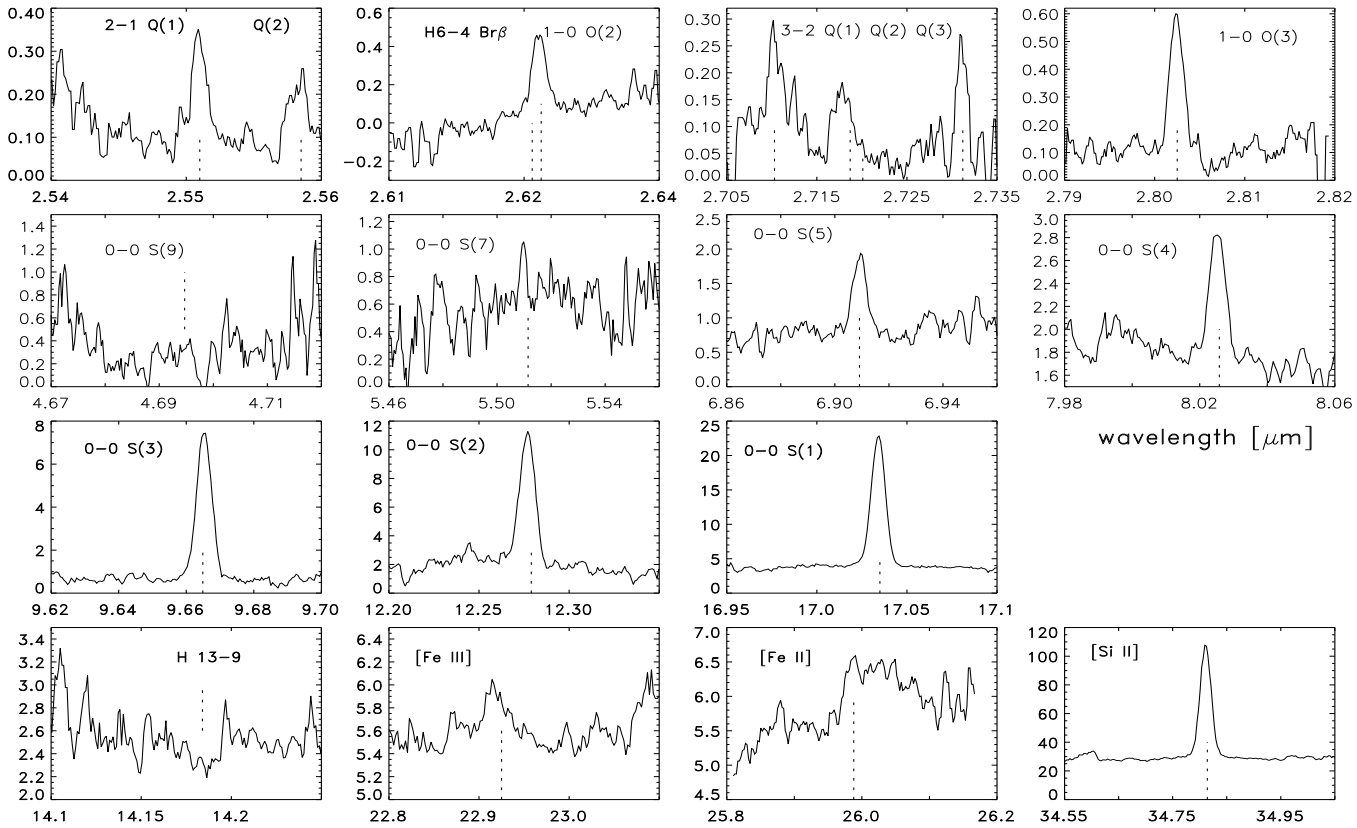

Fig. 2. ISO SWS spectra of lines scanned toward S140. Flux density is given in Jansky = 10^{-23}erg s^{-1}cm^{-2}Hz^{-1}.

2.1. Line flux and surface brightness

We have obtained spectra at 15 wavelength positions, aiming at prominent H_2 lines of $v = 0-0, 1-0, 2-1$, and $3-2$ transitions, one HI recombination line, and SiII, FeII, and FeIII fine structure lines. The 15 wavelength bands were each scanned at least four times for 100 seconds each scan in the AOT SWS02 mode. The integrated line fluxes were computed from the product of the peak line intensity above the continuum, and the observed full line width at half maximum, $\Delta V_{\rm obs}$. The observed surface brightness, $I_{\rm obs}$, of a line is the integrated flux, divided by the beam size. The systematic flux errors due to the present SWS calibration uncertainties are estimated as ±30%. Statistical errors were computed from the noise level near the line (setting 3σ to the average peak-to-peak amplitude variations), and are generally smaller than the systematic errors. To estimate an upper limit to an undetected line, we assume that a line with a 2σ peak flux would have been detected, so that its upper limit is 2σ times the expected FWHM due to instrumental resolution, $\Delta V_{\rm exp}$. The wavelength resolution ranges between 1000 and 2000 (cf. SWS observers manual).

For H_2, the apparent column density of an upper level is given by $N_{\rm app} = 4\pi\lambda\ I_{\rm obs}/(hcA)$. Because of extinction, the true column density, $N_{\rm obs}$, which is shown in Fig. 3, is larger. The interstellar extinction towards S140 we estimate from $E(B-V) = 0.60$ towards HD211880 (Hiltner 1956) and a standard extinction curve as $A_K = 0.21$. We assume a total $A_K = 0.3$ to allow for additional extinction within the inclined PDR.

2.2. Line detections

We detected twelve H_2 lines and derived upper limits for three more. The strong [SiII] 34.8141μm line was detected, and [FeII]25.988μm is marginally seen on a strong continuum. We found a line-like feature 100 km s^{-1} red of [FeIII]22.925μm. If we calculate the Fe abundance from the strength of this feature and the peak EM in the H^+ rim (§3.1), we find Fe/H $\simeq 3.5\times10^{-6}$, which is significantly larger than the 5.2×10^{-8} we derive from the [FeII]25.988μm line (§3.2). Although this might indicate that a substantial fraction of the Fe is returned from dust to gas by some unknown process when the grains are exposed to ionizing radiation and 10^4K plasma, much more likely the feature is an artifact.

H_2 1-0 O(2) may be blended with the HI $n = 6-4$ Brβ line at 2.6259μm, but from the peak EM in the H^+ rim and the Brβ/Hβ emission ratio of 0.0495 from Storey & Hummer (1995) we estimate $I(\mathrm{Br}\beta) \lesssim 4\times10^{-6}$ erg s^{-1}cm^{-2}sr^{-1} $<$ 10% of the observed flux. 2-1 Q(9) may be marginally (2σ) detected as a peak appears in the individual scans. 0-0 S(7) has a measured width of 150 km s^{-1}, although the instrumental resolution is 300 km s^{-1}. The line does appear to be there as it stands out in the individual scans. For lines where the observed and expected

Table 1. Observed lines

Line	$\lambda_{\rm rest}$ [μm]	[sec]	$I_{\rm obs}$ [10^{-5}erg/ s cm^{2}sr]	ΔV [km/s] obs / exp	E/k [K]
2-1 Q(1)	2.5510	600	2.05 - 2.42	137 / 150	11789
2-1 Q(2)	2.5585	600	1.31 - 1.12	177 / 150	12095
1-0 O(2)	2.6269	400	4.65	208 / 200	5987
3-2 Q(1)	2.7103	400	2.09 - 1.90	207 / 188	17098
3-2 Q(2)	2.7187	400	1.92 - 1.36	267 / 188	17387
2-1 Q(9)	2.7201	400	$\leq$0.32	– / 188	18107
3-2 Q(3)	2.7312	400	1.72 - 2.02	163 / 188	17818
1-0 O(3)	2.8025	400	5.45	201 / 176	6149
0-0 S(9)	4.6946	600	$<$1.44	– / 166	10262
0-0 S(7)	5.5112	400	1.9 - 3.8	153 / 300	7197
0-0 S(5)	6.9095	400	6.38	257 / 250	4586
0-0 S(4)	8.0251	400	4.10	211 / 200	3474
0-0 S(3)	9.6649	400	16.8	158 / 167	2503
0-0 S(2)	12.279	1200	19.7	238 / 231	1681
0-0 S(1)	17.035	600	19.8	160 / 167	1015
HI 13-9	14.183	600	$<$0.42	– / 200	
[FeIII]	22.925	400	0.61 ???	277 / 286	
[FeII]	25.988	400	0.56	– / 260	
[SiII]	34.814	800	30.2	207 / 250	

(due to instrumental resolution) widths are very disparate, we list a range of fluxes derived from either.

3. Discussion

Although B-type stars emit little ionizing Lyman continuum (Lyc) radiation, their strong far ultraviolet (FUV) emission can lead to significant emission of infrared radiation in surrounding photodissociated and heated molecular gas. In S140, the B0.5V star HD 211880 (spectroscopic distance $\approx$ 830 pc from m_V = 7.75 [Hiltner 1956], $M_V = -3.7$, and $A_V = 3.1 \times 0.60$) is embedded in a small HII region that is bounded north-eastward by dense molecular clouds. The cloud core nearest to the star has received considerable attention because it embeds a small group of strong infrared sources and a molecular outflow, and shows a prominent optically bright rim (Blair et al. 1978), indicating that it is being photoevaporated and dissociated by the B star; the sharp transition between the dark cloud and the ionized gas seen at optical and radio (Falgarone & Gilmore 1981; Schwartz 1985; Evans et al. 1987) wavelengths suggests that the line connecting the star and cloud is approximately in the plane of the sky.

The FUV radiation in the range 912-1110Å photodissociates a surface layer of the molecular cloud in which the gas is heated to temperatures in the range $10^2 - 10^3$ K and emits strong IR radiation. The structure and emission of such a PDR is mostly determined by the gas density, temperature, and the incident FUV flux (Black & van Dishoeck 1987; Sternberg 1988; Sternberg & Dalgarno 1989; Hollenbach et al. 1991; Draine & Bertoldi 1996).

3.1. Gas density in the PDR

To estimate the gas density in the PDR we can assume that the PDR is in pressure equilibrium with the ionization front (IF). In the bright rim near the IF the observed peak 21 cm flux density observed by Falgarone & Gilmore (1981) of 4 mJy/beam (25″ beam) yields an emission measure of $\sim$ 2200 pc cm^{-6}, which for a pathlength of $\sim$1 pc gives an electron density of about 45 cm^{-3}. From the integrated flux of 150 $\pm$ 60 mJy (Evans et al. 1987 derive 130–150 mJy) and $T \approx$ 8000K we derive a total number of recombinations of 7×10^{45}s^{-1}. In the radio map of Evans et al. the ionized rim has an opening angle of about 50° as seen from the B star, so that for an axisymmetric shape around the line connecting the star and cloud, the star's total Lyc emission becomes $S_{ly} \approx 1.8 \times 10^{47}$s^{-1}.

We combined Kurucz ATLAS 9 and Kunze (1994) non-LTE stellar atmosphere models with the stellar evolution models of Schaller et al. (1992), and found a $T_{eff} \simeq$ 29000 K, $L_{bol} \simeq 3.1 \times 10^4 L_\odot$ model to best match the observed, dereddened UBV magnitudes. This model yields $S_{ly} \approx 1.0 \times 10^{47}$s^{-1}, in reasonable agreement with the radio estimate; in the 912-1110Å range, $S_{uv} \approx 1.6 \times 10^{48}$s^{-1}.

With an angular separation of 7′ (R = 1.7 pc) between the star and the cloud surface, the density of ionized gas right at the IF can be estimated as $n_i = S_{ly}/(4\pi R^2 q c_i) \simeq 40\ S_{ly,47}^{1/2}$ cm^{-3} (Bertoldi & Draine 1996), where $q \simeq 6.5 S_{ly,47}^{1/2}$ is the factor by which the ionizing radiation is attenuated in the evaporation flow (Bertoldi 1989), and c_i is the isothermal sound speed in the gas. This density agrees with that derived from the peak 21 cm flux density, and yields an independent check for the atmosphere model we use to estimate S_{ly} and S_{uv}.

Pressure balance across the IF, $2 n_i c_i^2 \simeq n_{pdr} \sigma^2$, now yields the density in the PDR as $n_{pdr} \simeq 10^4 \sigma_5^{-2} S_{ly,47}^{1/2}$ cm^{-3}, where σ is the velocity dispersion of the gas in the PDR. We thus expect the gas density in the PDR to be of order 10^4 cm^{-3} for a typical $\sigma \simeq 1$ km s^{-1}. The gas pressure we thus estimate in the PDR, $P/k \simeq 2 \times 10^6$ cm^{-3}K is comparable with that inplied by the density measured in the molecular gas of the L1202/L1204 cloud (e.g., Ungerechts et al. 1986; Hayashi & Murata 1992).

3.2. Comparison with PDR models

We constructed plane-parallel models of the PDR in S140 using the method described in Draine & Bertoldi (1996) to match the SWS observations. A comparison with models computed following Sternberg & Dalgarno (1989, 1995) shows minor quantitative differences. The result of a good model fit is shown in Fig. 3. In this model we assumed a gas density of 10^4 cm^{-3} and an incident 912-1110Å FUV flux of χ = 400 times the photon flux of a Habing field (1.23×10^7cm^{-2}s^{-1}), which is the flux expected at 1.7 pc from a star with $S_{uv} = 1.6 \times 10^{48}$s^{-1}. A dilute black body incident spectrum was assumed, and a temperature profile T = 20K + $(T_0 - 20\text{K})/(1 + 50\tau_{d,1000}^2)$, where $\tau_{d,1000} = 6 \times 10^{-22} N_{\rm H}$ (Bertoldi & Draine 1996) is the dust optical depth at 1000Å from the PDR surface to a position within it. The temperature profile was chosen such that T drops in the transition region from atomic to molecular hydrogen. We searched for values of T_0 and the inclination angle of the PDR normal to the line of sight, θ, for which the model column densities best match those observed. Good agreement was reached

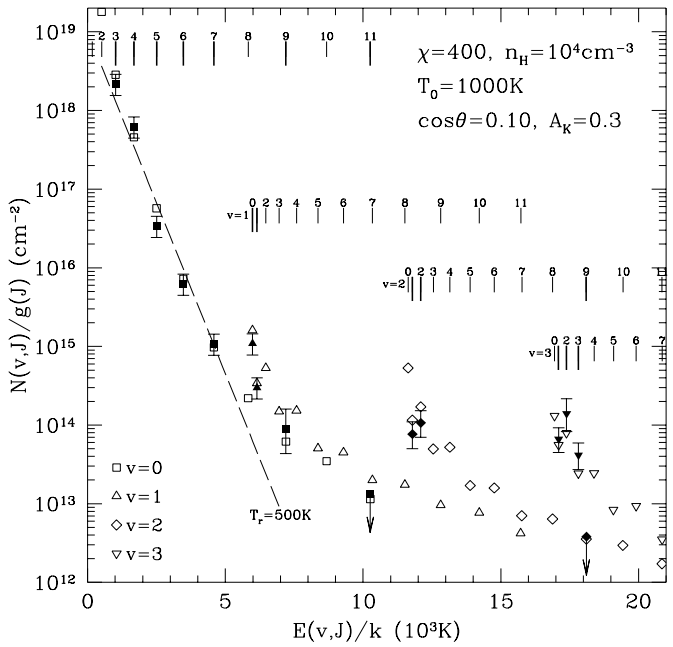

Fig. 3. *Above:* Observed (filled symbols) and model (open symbols) column densities in the ro-vibrational levels of H_2. A simple fit to the low v = 0 levels suggests a temperature of ca. 500 K. *Below:* Atomic and molecular hydrogen abundance in our model PDR, and the adopted temperature profile.

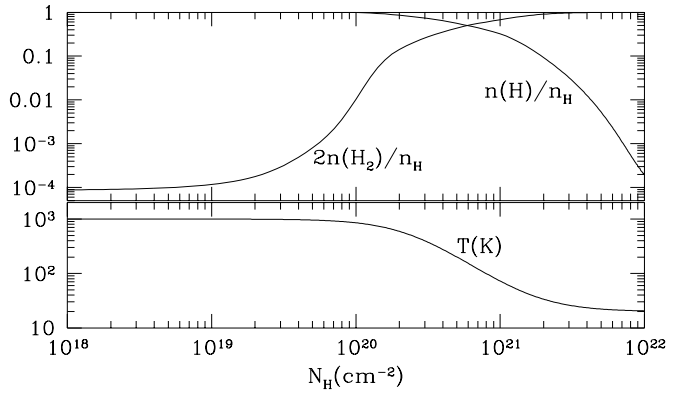

with T_0 = 1000K and $\cos\theta = 0.1$. The apparent rotational temperature of the observed v = 0 levels is $\approx$ 500 K. However, at 10^4 cm^{-3} the density is not high enough to thermalize the populations in $J \geq 5$, so that we were led to adopt a non-uniform temperature structure in our model.

We computed the fine structure emission expected from our inclined model PDR following the approach of Tielens & Hollenbach (1985) and find I_{obs}([SiII]35μm) = 1.9×10^{-4} erg s^{-1}cm^{-2}sr^{-1}, and I_{obs}([FeII]26μm) = 1.4×10^{-5} erg s^{-1}cm^{-2}sr^{-1}, assuming ζ Oph depletion: Si/H= 9×10^{-7} and Fe/H= 1.28×10^{-7}. Our model would agree with the observations if the silicon abundance was 1.6 times that toward ζ Oph, and the iron abundance was 0.41 that toward ζ Oph. Since we do not know the abundances in dense clouds accurately (the cloud toward ζ Oph has much lower density), the abundances which we would infer from these observations are not unreasonable. We must also keep in mind that the available collision rates for FeII excitation are very uncertain.

Our model predicts I_{obs}([CI]609μm) = 8.8×10^{-6} erg s^{-1}cm^{-2}sr^{-1} (C/H= 1.4×10^{-4}), close to the observed $8.7 \pm 0.7 \times 10^{-6}$ erg s^{-1}cm^{-2}sr^{-1} of Minchin et al. (1994) with a 10″ beam. Our predicted I_{obs}([CII]158μm) = 9.6×10^{-4} erg s^{-1}cm^{-2}sr^{-1} is about twice of what Schneider et al. observed at this location with a 55″ aperture; beam dilution may well be responsible for the discrepancy. Our model predicts strong I_{obs}([OI]63μm) = 6.9×10^{-3} erg s^{-1}cm^{-2}sr^{-1} (O/H= 3.2×10^{-4}), which is about eight times of what Schneider found with a 22″ aperture. We further predict I_{obs}([OI]145μm) = 2.9×10^{-4} erg s^{-1}cm^{-2}sr^{-1}, and for H_2 0-0 S(0), I_{obs} = 1.5×10^{-5} erg s^{-1}cm^{-2}sr^{-1}.

Acknowledgements. We thank A. Natta, M. Walmsley, N. Schneider, D. Hollenbach, and P. Reich for valuable comments. This research was supported in parts by a grant from the DFG, by NSF grant AST-9219283, and by the German-Israel Foundation grant I-196-137.7/91. SWS and the ISO Spectrometer Data Centre at MPE are supported by DARA under grants 50 QI 8610 8 and 50 QI 9402 3.

References

Bertoldi, F. 1989: ApJ 346, 735
Bertoldi, F., Draine, B. T.: 1996 ApJ 458, 222
Black, J.H., van Dishoeck, E.F.: 1987 ApJ 322, 412
Blair, G.N., Evans, N.J., Vanden Bout, P.A., Peters, W.L.: 1978 ApJ 219, 896
Draine, B.T., Bertoldi, F.: 1996 ApJ 468, 269
Evans, N.J., Kutner, M.L., Mundy, L.J.: 1987 ApJ 323, 145
Falgarone, E., Gilmore, W.: 1981 A&A 95, 32
Hayashi, M., Omodaka, D., Hasegawa, D., Suzuki, S.: 1985 ApJ 288, 170
Hayashi, M., Hasegawa, D., Omodaka, D., Hayashi, S.S., Miyawaki, R.: 1987 ApJ 312, 327
Hayashi, M. & Murata, Y.: 1992 PASJ 44, 391
Hiltner, W.A.: 1956 ApJ Suppl. 2, 389
Hollenbach, D., Takahashi, T., Tielens, A.G.G.M.: 1991 ApJ 377, 192
Kunze, D.: 1994, PhD Thesis, Munich University
Minchin, N.R., White, G.J., Padman, R.: 1993 A&A 277, 595
Minchin, N.R., White, G.J., Stutzki, J., Krause, D.: 1994 A&A 291, 250
Minchin, N.R., Ward-Thompson, D., White, G.J.: 1995 ApSS 224, 203
Schaller, G., Schaerer, D., Meynet, G., Maeder, A.: 1992 ApJS 96, 269
Schneider, N., Krause, D., Johnen, C., Stutzki, J.: 1992 Astronomische Gesellschaft, Abstract Series, 7, 82
Schwartz, P.R.: 1985 ApJ 298, 292
Sternberg, A.: 1988 ApJ 332, 400
Sternberg, A., Dalgarno, A.: 1989 ApJ 338, 197
Sternberg, A., Dalgarno, A.: 1995 ApJS 99, 565
Storey, P.J., & Hummer, D.G.: 1995 MNRAS 272, 41
Tielens, A.G.G.M., Hollenbach, D.: 1985 ApJ 291, 722
Ungerechts, H., Walmsley, C.M., Winnewisser, G.: 1986 A&A 157, 207
White, G.J., Padman, R.: 1991 Nature 354, 511